Research Journal of Applied Sciences, Engineering and Technology 3(6): 474-485, 2011
ISSN: 2040-7467

Received: December 01, 2010 Accepted: December 30, 2010 Published: June 25, 2011

Mechanical Performance of Polyisoprene used in Building a Flapping Foil Underwater Robot

M.O. Afolayan, D.S. Yawas, C.O. Folayan and S.Y. Aku
Mechanical Engineering Department, Ahmadu Bello University, Zaria

Abstract: Imitating living object mechanically is the current trend in the frontier of robotics. A better imitation is assured if the material used for the joints is a biological equivalent. Polyisoprene (Natural Rubber) has some physical properties that is close to muscle material and is thus presented in this work. The problem of it becoming soft as it get involved in repetitive task of oscillation and bearing weights of attached part led to designing a dedicated testing machine to find out the rate not to exceed. The rubber sample used was found to show significant softening at frequency of 25 Hz. The polyisoprene material was used to build simple planar joint and adapted for flapping foil underwater robot in the form of a Mackerel robotic fish (394.01 mm long). A test at frequency of 2 Hz (an average swimming value) works perfectly well - it has proper kinematics as that of a living fish.

Key words: Biomimetic, elastomer, fish robot, hyper-redundant robots, rubber

INTRODUCTION

Robotics is the science and technology of robots, their design, manufacture, and application. Robotic researches are either abstract or biomimetic (biologically inspired). The biologically inspired robots imitate some characteristics of life forms such as mobility (Rodney, 1989a, b), vision (Zufferey and Floreano, 2005), Harrison and Koch, 2000; Brett *et al*., 2003; Srinivasan, 1992), flying (Zufferey and Floreano, 2005; Srinivasan *et al*., 2004) and navigational methodology (Park *et al*., 2007). Biomimetic systems are greatly desired because natural systems are highly optimized and efficient. Srinivasan (1992) calls them shortcuts to mathematically complex issues of life. Take a look at fly or honey bee, they have very small brain and processing power but no literature has a robot with such visual capabilities like them. Nearly all the five senses of living being i.e. sight or vision (Zufferey and Floreano, 2005; Srinivasan *et al*, 2004), hearing and touch (Anonymous, 2010a, b), smell Grasso (2000) and taste (Anonymous, 2010c) are imitated. Zufferey and Floreano (2005) semi-autonomous indoor airplane was only possible because of its biomimicry. The abstract ones are designed to solve a specific problem and mostly use the most sophisticated and expensive hardware available. Of this categories are industrial assembly robots. Their design is direct solution to problem ahead without attempt to shortcut it, i.e. formal methods and formal specification are used for designing such robots especially where safety and no failure is important.

To improve intelligence, knowledge database with inference engine for artificial intelligent programmes exist such that people all over the world can contribute their common knowledge. Example is Cyber Corps (CYC) located at http://www.cyc.com/ and is supported by several companies such as Microsoft, Apple, Bellcore, Digital Equipment Corporation, US Department of Defense, Interval, and Kodak.

Hyper-Redundant Robots (HRR) are robots in the form of serpentine or snake or rod shape. Tentacle, Trunk, Fish are examples of biological hyper-redundant body. The redundancy means different ways to perform the same movement and is usually denoted in terms of degrees of freedom.

A rod shape robot have these advantages:

- The redundancy will allow them to still function after losing mobility in one or more sections
- Stability on all terrain because of low center of gravity
- Terrainability which is the ability to traverse rough terrain
- Traction is very high as the whole body is involved
- Efficiency in energy use as there is no need to lift the body off ground
- Small size that can penetrate small crevices

The disadvantages include difficult control system for the several degrees of freedom joint, low speed and problematic thermal control (Kevin, 1997) because of low surface to volume ratio.

Examples of scenario where Hyper-Redundant Robots can serve are:

- under water devices (military -search and defenses, civilian - Oil installation, oil platform superstructure inspection in real time, fish decoy)

Corresponding Author: M.O. Afolayan, Mechanical Engineering Department, Ahmadu Bello University, Zaria

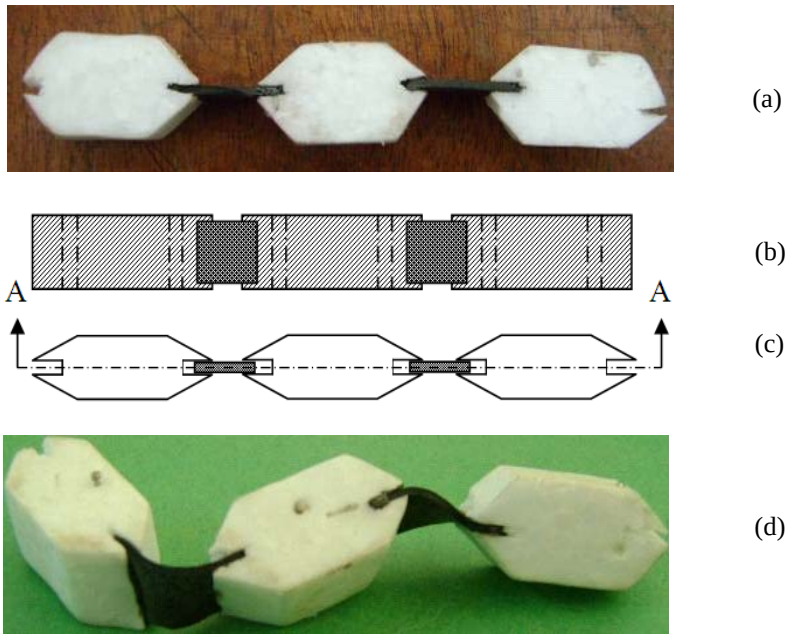

Fig. 1: (a) The developed robotic joint; (b) cross-section; (c) top view; (d) and isometric view showing twist and bending

- search and rescue among rubbles, cheap and distributed space exploration (Anonymous, 2008a)
- fire fighting (as intelligent fire hose (Anonymous, 2008b))
- manufacturing and machine maintenance in a convoluted environment (Matsuura *et al*., 1985)
- medical science - minimally invasive surgery
- military purposes e.g. Espionage, Surveillance, Bomb disposal
- others are pipe inspection, stealth perimeter surveillance and guarding

Statement of the problem: Control has been one of the tasking issues in the development of hyper-redundant robots. Biological hyper-redundant bodies like worms and caterpillars have small brain and can still work perfectly and efficiently in a 3D world. It means there are shortcut (Gutfreund *et al*., 1996) nature is using (though varied) to implement this complex control strategy (Yekutieli *et al*., 2005, 2007; Gutfreund *et al*., 1998; Shammas *et al*., 2003). The problem then is how can a better biomimicry be done in designing an hyper-redundant joints that will allow the use of control strategy close to that of nature.

Biological HRR systems have *almost* a continuum body, for example, snakes have over 200 vertebrate (200-1 joints) to support its body. An elephant trunk have no single joint in it trunk, worms have no joint also. Most researchers have being extrapolating convectional joints - hinge, universal, even ball and sockets in trying to build hyper-redundant robots for example Shammas *et al*. (2003). A solution is to use a non living material with behaviour close to the biological model.

Biological materials stress-strain relationship have been treated and shown to be hyper lastic in nature (Dorfmann *et al*., 2007). The stress-strain behaviour is the same with some elastomers. For examples, Neo-Hookean and Fung-elastic exponential model have been used to model elastin (Wikipedia, 2008) while *manduca sexta* (tobacco hornworm butterfly caterpillar) muscles was modeled by Dorfmann *et al*. (2007) using Ogden and Roxburgh (1999) hyper elastic model. Furthermore, carbon filled natural rubbers have been shown to have very close mechanical properties to living tissues (Dorfmann *et al*., 2007).

Rubber has among its other natures the mechanical softening effect under dynamic loadings (Ogden, 2000; Miller and Arbor, 2008). Using it for building hyper-redundant robots by imitating hydrostatic bodies like worm and caterpillar requires the knowledge of this softening effect as continuous bending, stretching and tensioning is commonly experienced in such body.

Description of the robotic joint: Figure 1 shows the basic form of the hyper-redundant robotic joint that was developed; it is a device with intersegment revolute joint made up of carbon filled rubber stripes cut from motor car inner tube. The rubber will allow movement other than planar motion without much complicated design. The rubbers also act as a restoring spring when actuating load is removed. Figure 2 is a practical implementation of the joint for a fish like robot tail. The segments are cable controlled while the rubbers act as a restoring load.

The objective of study: The objective of this study is to experimentally find out what frequency will softening

Fig. 2: A robotic fish tail using rubber for its joint - the rubber simplifies its control scheme, maintain the rigidity and restoring force and allows the wave like swimming action of the tail section

becomes a limiting factor. This work also aim at using only one manufacturer product since the compounding material used for the rubbers will definitely give different result, in other word, the same product tested will be used for the building of the robot joint.

Rubber testing: Rubber and other elastomers are generally tested using Dynamic Mechanical Analyzer. The rubber sample is subjected to oscillation (usually sinusoidal) while the cooled sample is gradually heated up. The oscillation frequency and the heating process are normally varied in a stepwise manner. Thermomechanical properties like storage modulus and loss factors are derived in the process. The samples are normally tested for example in biaxial, uniaxial, multiaxial mode in compressive and tensile loading. The configuration selected usually reflect the mode the final product will be while in service.

MATERIALS AND METHODS

Sample description: A rubber sample in the form of inner tube of cars (14 inch rim) made by Kings rubber company in China was procured and cut into strips of 20 mm x 10 mm. The tube is 1.5 mm thick and is made up of natural rubber. The rubber samples were pre-stressed by extending to 200% and relaxing them 30 times. Furthermore, they were allowed to stabilize geometrically and thermally before proceeding with the test.

Description of the frequency loss pattern machine: The test equipment was designed to test rubber in cantilever mode. Figure 3 shows the equipment consisting of data logger, linear motor driver, test board and precision signal generator.

The test board (Fig. 4) consists of a linear motor, displacement sensor, thermocouple junction, and load sensor. The motor driver electronics is on a separate board. The sample is held in place by the clamp while the linear motor oscillates at a frequency determined by the pulse rate from a power amplifier connected to the computerized signal generator. The plastic strip holding the rubber sample is not transparent in some part (about

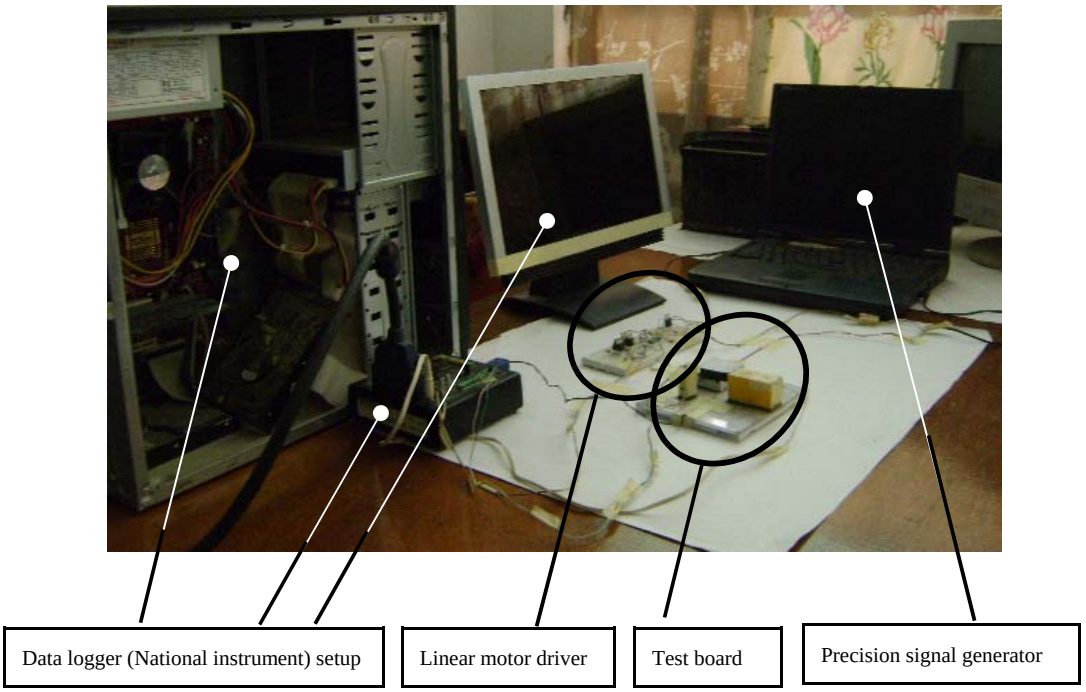

Fig. 3: The frequency loss determination equipment

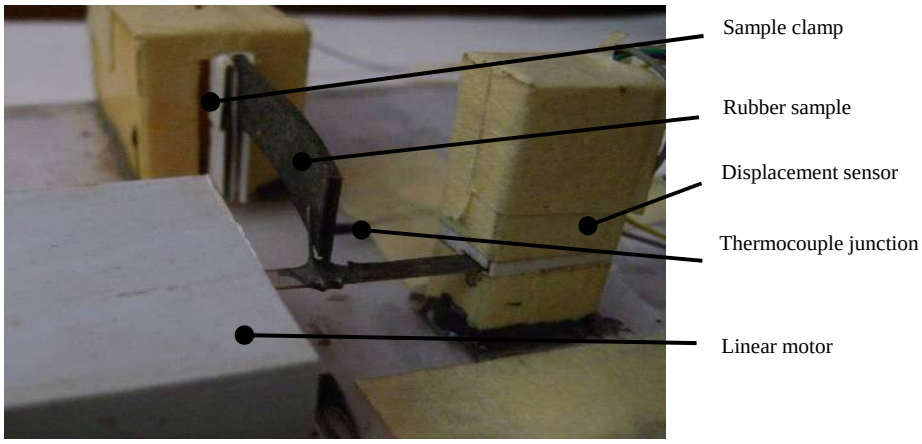

Fig. 4: Closer view of the test board

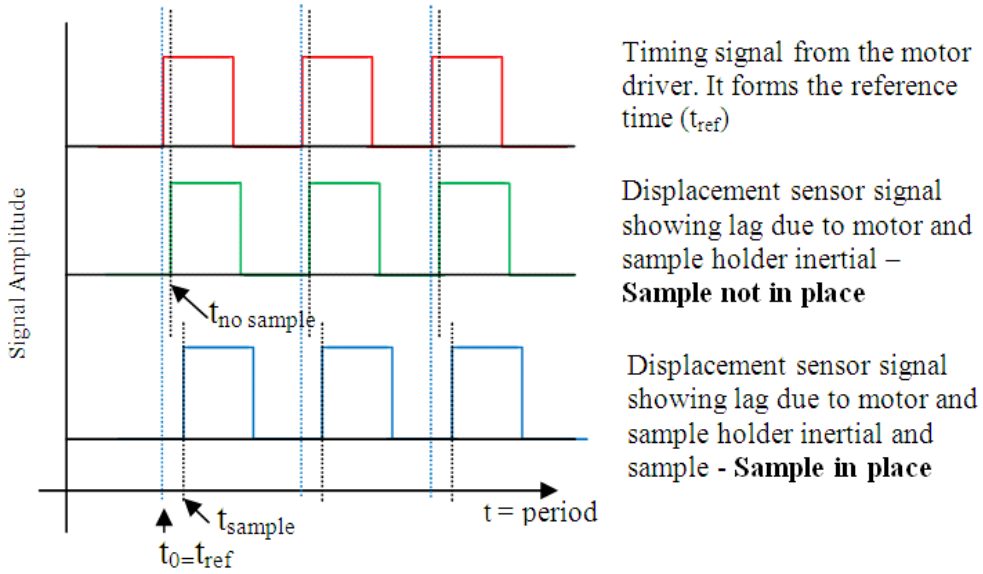

Fig. 5: Signal pattern showing presence and absence of sample rubber. The delay is increased when sample is in place. The absolute value of this delay is obtained from t_{sample} - $t_{no\ sample}$ - t_{ref}

two third) so that when it moves in and out, it activates the photocell and makes it to generate an on-off signal. The signal accessory (Fig. 12) captures all the voltage levels from the signal generator, linear motor, photocell, thermocouple junction nearby and even the sample holder (that has built in piezo sensor). The really critical signal is outline in Fig. 5. The delay in signal is a function of the property of the rubber and the frequency of the oscillation. The amplitude of the signals are not so relevant but the timing.

Design of the linear motor: The linear motor provides the motive force for the oscillatory motion. Figure 6 and 7 shows the assembly drawing of the motor and the semi darkened polystyrene plastic stripe which it use for holding sample and modulating the photocell.

This design approach greatly reduces inertial by using light weight materials copper coil without iron core (~43.0 mg) and polystyrene plastic (~1.0 mg). It was tested and found to be capable of oscillation greater than 50Hz. Its speed is precisely controlled by the computerized motor driver. The motor driver interfaces with the Spectral Plus 5.0 software that generate the timing signal. The motor driver (Fig. 8) is controlled by pulses from the computer sound card line out port which it convert to alternating square wave signal using 4027 J-K flip flop bistable multivibrator. The 4027 bistable multivibrator drives power transistor bridge to which the

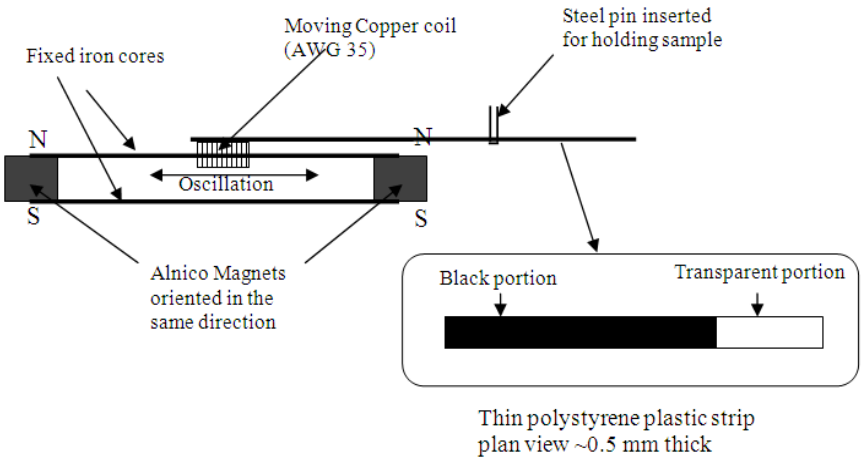

Fig. 6: Linear motor design and its component

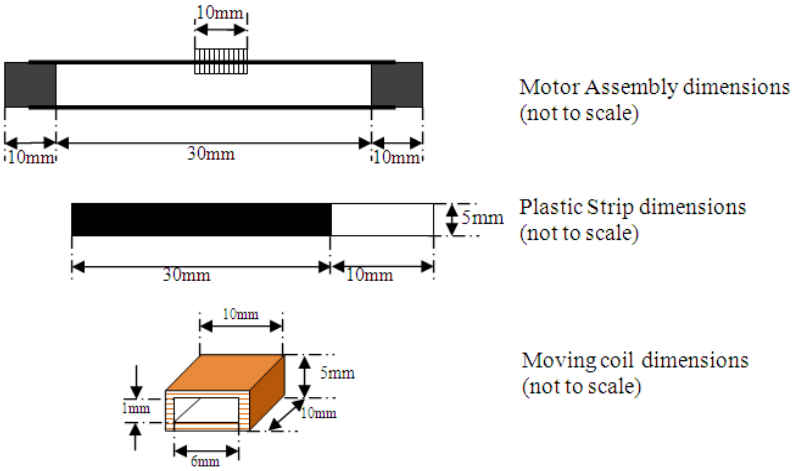

Fig. 7: Linear motor components dimensions

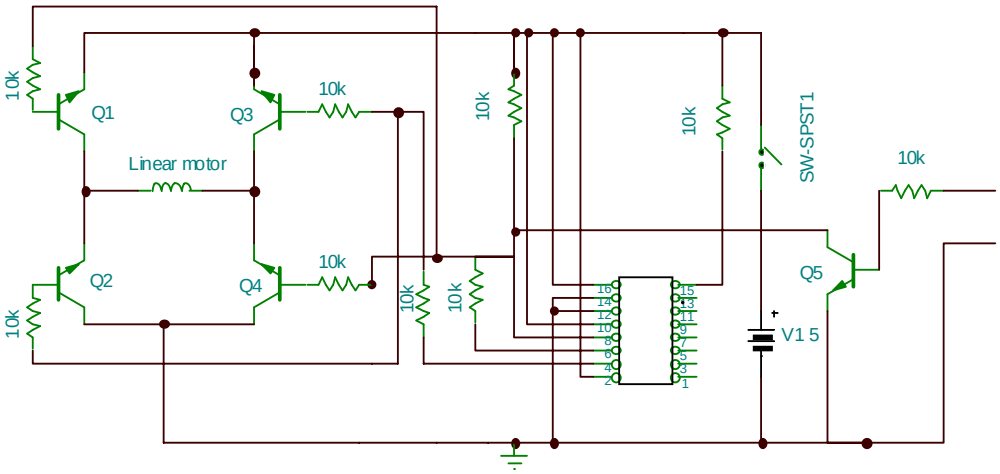

Fig. 8: Circuit diagram of the motor driver

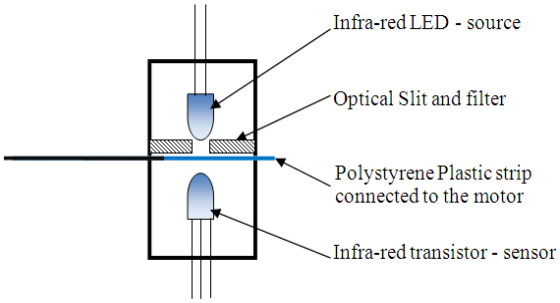

Fig. 9: Internal design of the displacement sensor

motor coil is connected. The square wave signal has 50% duty cycle.

Although the signal input to the motor (and hence the rubber sample) is square wave, the actual influence on the sample is rather like a shock load or technically an impulsive loading. This is more so for the fact that the rubber response is much more slower than the slew rate of the motor <20 ms and the period of measurement is also very short (the time it takes for the photocell to signal block its light path). Also if the rubber sample is approximated by a linearly damped-mass-spring body (voigt body), the impulsive input implies that its response will give its dynamic characteristic (Katsuihiko, 2005; Nagrath and Gopal, 2005). For linear-time-invariant system (for which is an approximation in this scenario), the impulsive response is given by:

$$C(s) = G(s)R(s) = G(s)$$

where $L\ \delta(t) = 1 = R(s)$ and transfer function = $C(s)/R(s) = G(s)$, Therefore,

$$c(t) = L^{-1}G(s) = g(t)$$

and using convolution integral:

$$c(t) = \int_0^t g(t-\tau)r(\tau)d\tau$$

the system's response can be found to any input (Katsuihiko, 2005; Nagrath and Gopal, 2005). Summarily, driving the sample with square wave signal allows the rubber to give realistic response that is a function of its nature.

Design of the displacement sensor: This uses photocell (Fig. 9) to measure the reaction time of the sample, header and the motor. The reaction time measured is rather

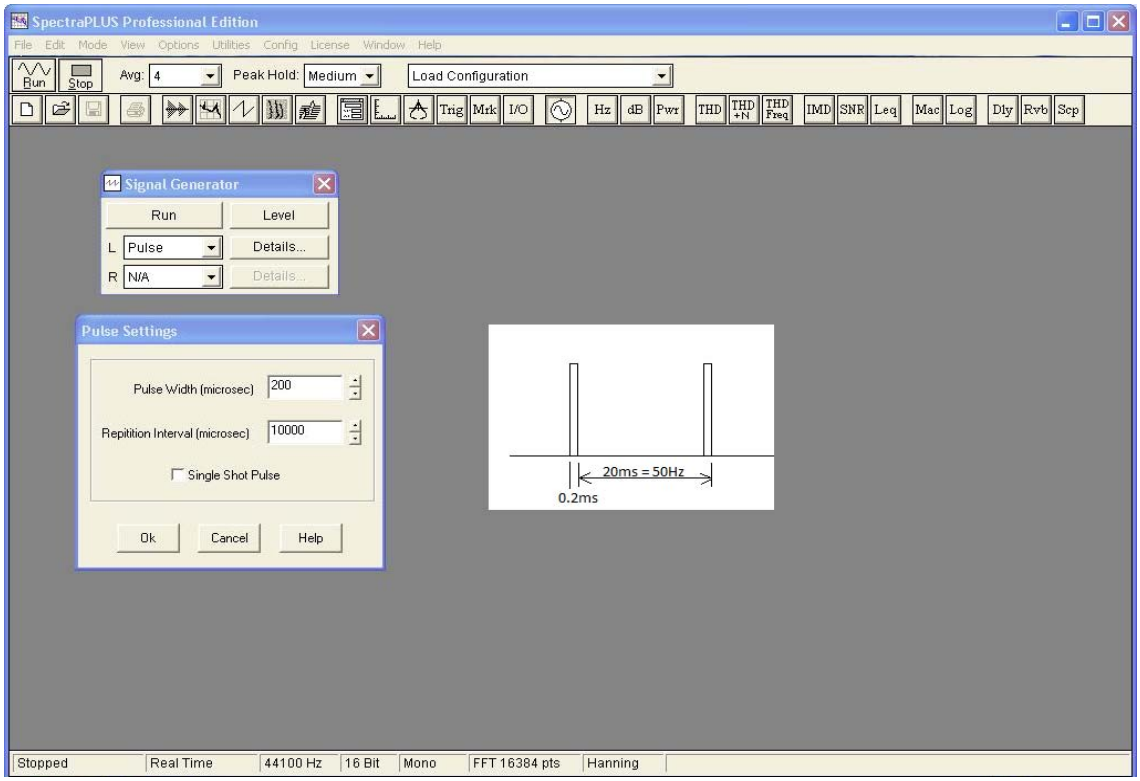

Fig. 10: The Spectral Plus 5.0 Signal Generator software interface showing the dialog boxes for the signal frequency and type setting. Inset is the timing for the selected setting

relative that is, it sends signal to the data logger as soon as its light path is blocked without recourse to how long the motion was started. This design is used instead of absolute reaction time to reduce measurement error. The plastic strip has to travel the same distance for it to block the light. The time the signal generator sends its signal and the time the photocell sends signal is a function of the sample (rubber) stiffness, the stiffer the rubber, the longer the lagging of the photocell signal behind the motor signal (t_{ref} of Fig. 5). The accuracy of the measurement is thus left to the National Instrument PCI data logger built in timing facilities (which is already factory calibrated).

Thermocouple junction: A Nichrome-Constantan thermocouple junction is placed near the sample (within 1 cm) so as to measure the environmental temperature while the experiment is going on. The National Instrument Data Signal Accessories used in this experiment provides built in cold junction and all the necessary compensation required. The sample was temperature stabilized using fan before each experiment.

The sample clamp: has built in force sensor using piezoelectric plate for its transducer. The clam was not designed to measure the absolute force (as a function of the sample stiffness) and was neither calibrated. Its function is to act as a double check on the photocell reaction response in case it misses any data point for whatever reason. It might be possible to deduce parameters like shear complex, phi or loss angle of the sample if calibrated.

Computerized signal generator: The signal generator uses Spectral Plus 5.0 software (Fig. 10 is the interface) for its precision signal source. It is hosted on Dell Latitude CPt S500GT laptop with these specifications: BIOS - Phoenix ROM BIOS PLUS Version 1.10 A05, OS - Microsoft XP Professional Version 2002 with service pack 2, DirectX Version 9.0c, RAM - 192MB, Microprocessor - Intel Celeron 498MHz, Display Resolution (used) - 1024×768 (32bit),Sound Card ESS Maestro 3PCI, Sound Driver es198x.sys

The signal generator output is via the line out port which is then amplified using power amplifier to drive the linear motor. The signal pattern is pulsed with fixed width of 0.2 ms (200) for all the frequency used for the experiment.

Data logger and signal accessories: The National Instrument VI logger (Fig. 11 and 12) was hosted on Mercury Model P25G System with the following specification: BIOS - American Megatrends Inc 080012, 12/28/2005, OS - Microsoft XP Professional Version 2002 with service pack 2, DirectX Version 8.1, RAM - 256MB, Microprocessor - Intel Pentium 4 1.80GHz, Display Resolution (used) - 1280×1024 (32bit).

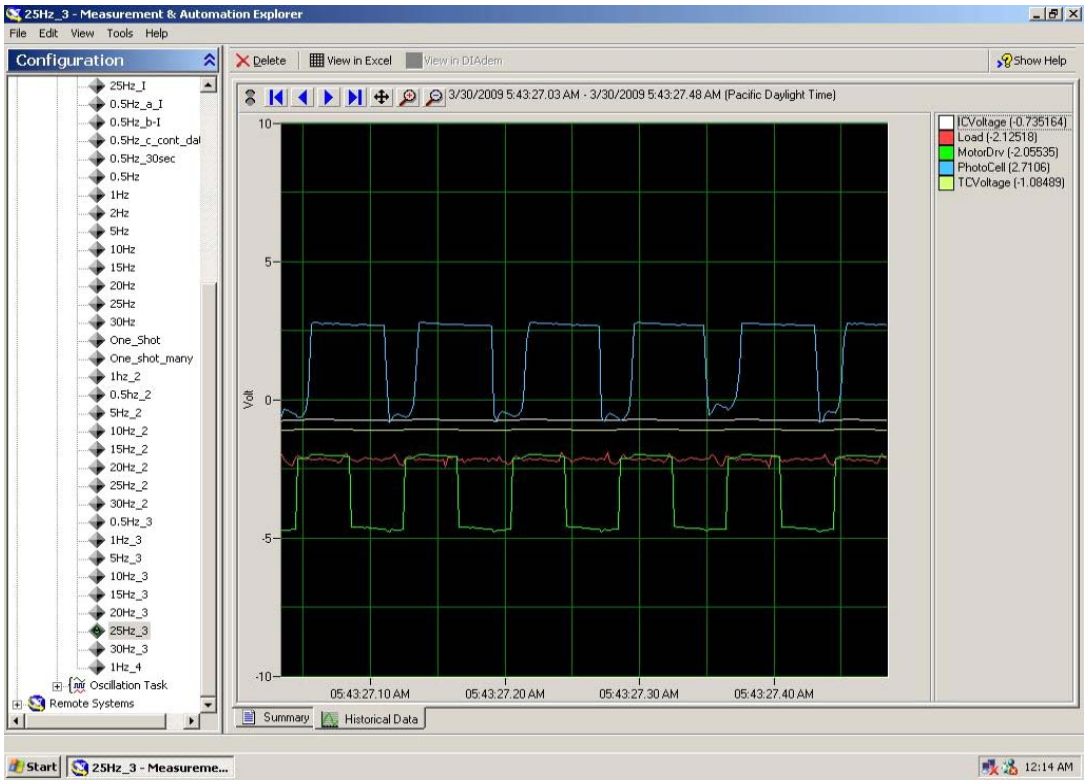

Fig. 11: National Instrument VI Logger interface - showing result at 25Hz input frequency

Fig. 12: The DAQ Signal Accessories (Left) interfaced to a computer (Right)

The data logger has capability to export the data in different file format for further processing on different software. CSV format was used in this project and further data mining was done using MS Excel 2003.

Experimental procedure: The samples were tested three times under the following conditions:

- Frequency: The frequency of oscillation was set to 0.5, 1, 5, 10, 15, 20, 25Hz and also at 30Hz.
- Temperature: Temperature was logged throughout the experiment The sample was stabilized first by moving air current over it using fan. A digital Nichrome-Constantan thermocouple thermometer was used to verify that the environmental temperature is stable.

Possible sources of error in measurement and the precautions taken:

Timing errors caused by motor inertia: As earlier written, absolute timing was not used but the relative time lag. It means motor lag will be constant as long as:

- the supply current to the windings is constant
- the weight of the coil and the plastic holder is constant i.e., the plastic is not being eroded by the oscillatory motion

Pulsing the motor winding at very small interval removes the first problem. The use of plastic member for the parts the plastic strip glides over (only one, at the entrance into the photocell casing) ensure reduced erosion and thus weight loss.

Furthermore the use of very light weight material for this moving part ensure that they can follow the input signal in a timely manner. The motor was tested and found to be capable of oscillations greater than 50Hz (reaction time of $\leq$20 ms) which is much greater than the frequency range 30Hz (Period T = 33.33 ms) used in this experiment.

Analog-digital conversion time: The NI PCI 1064 D/A conversion card to which the DAQ Signal accessories is connected to is a 16 channel device capable of 20Mhz conversion rate multiplexed between the channels. That is approximately 1.25 Mhz per channel, this is more than adequate for this work.

Out of synchronization error due to signal generator and the recorded values by the data logger: This is solved by recording the signal generator output and using it as the reference (Fig. 5) for all other values. It was found that this lag is constant and can thus be treated as a bias.

Temperature: has very serious influence on the property of elastomers, even filled ones. Compounding, vulcanization and filling reduce this influence as much as possible. The environmental temperature was stabilized using fan and the experiments were performed quickly-each requiring about a minute to do. The maximum temperature variation between the experiments is 1.1ºC

RESULTS AND DISCUSSION

Figure 13 to 20 shows the lags due to the rubber stiffness at various experimental frequencies used. Three

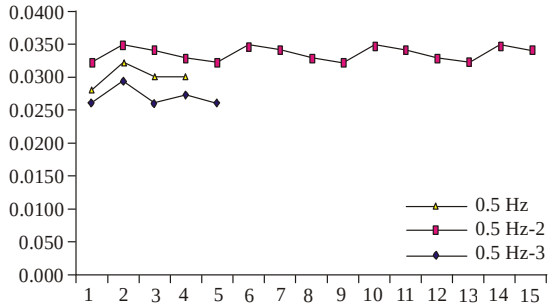

Fig. 13: Lag at 0.5Hz frequency of oscillation

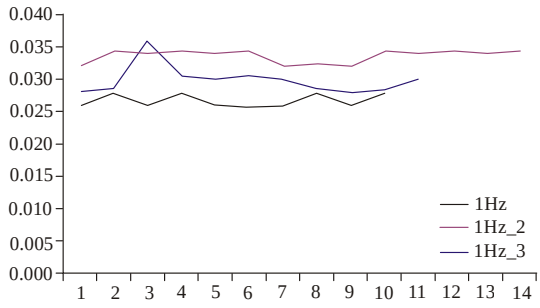

Fig. 14: Lag at 1 Hz frequency of oscillation

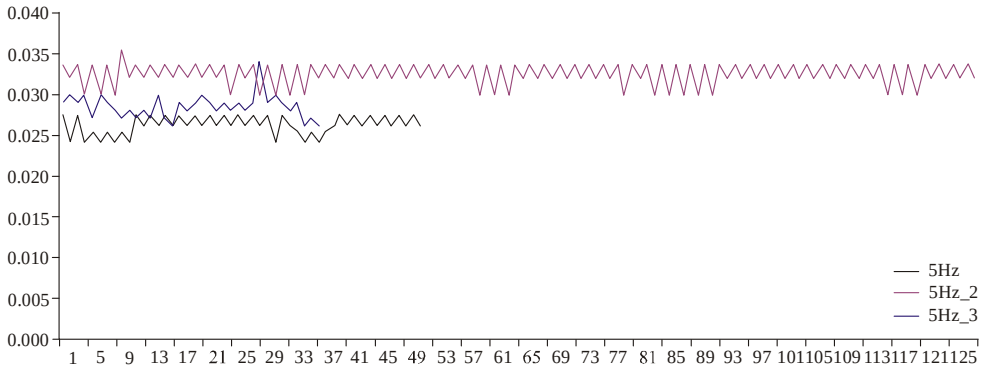

Fig. 15: Lag at 5Hz frequency of oscillation

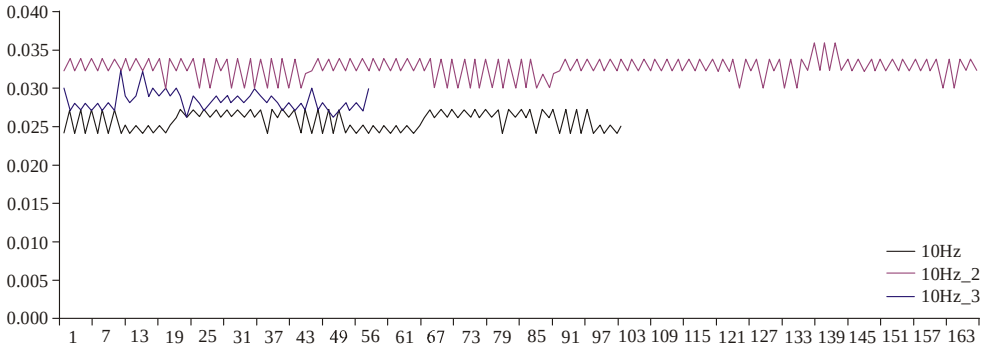

Fig. 16: Lag at 10 Hz frequency of oscillation

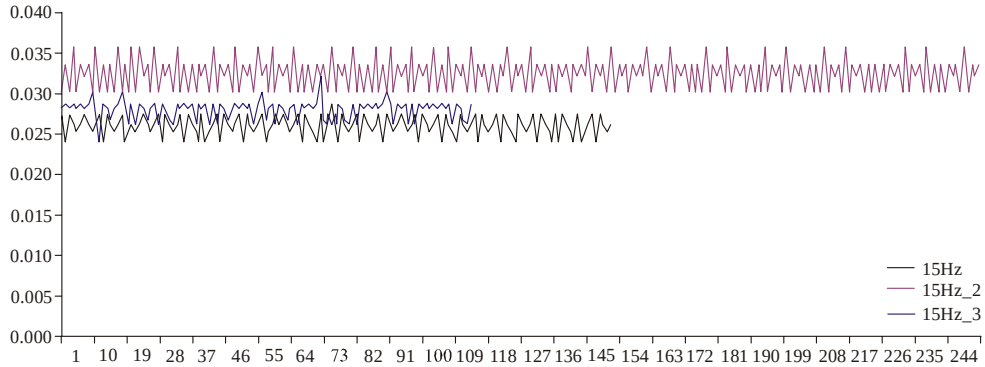

Fig. 17: Lag at 15Hz frequency of oscillation

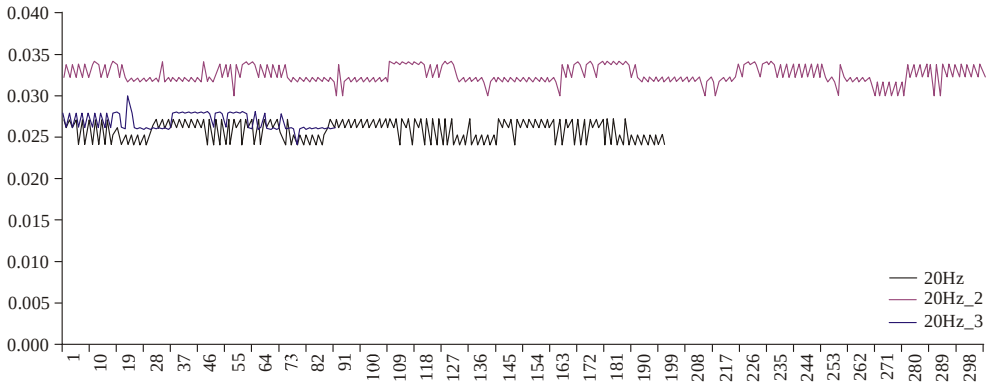

Fig. 18: Lag at 20Hz frequency of oscillation

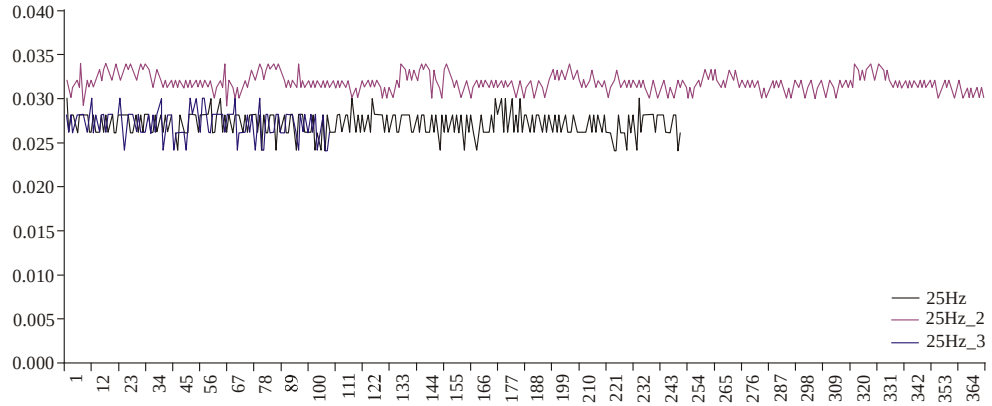

Fig. 19: Lag at 25Hz frequency of oscillation

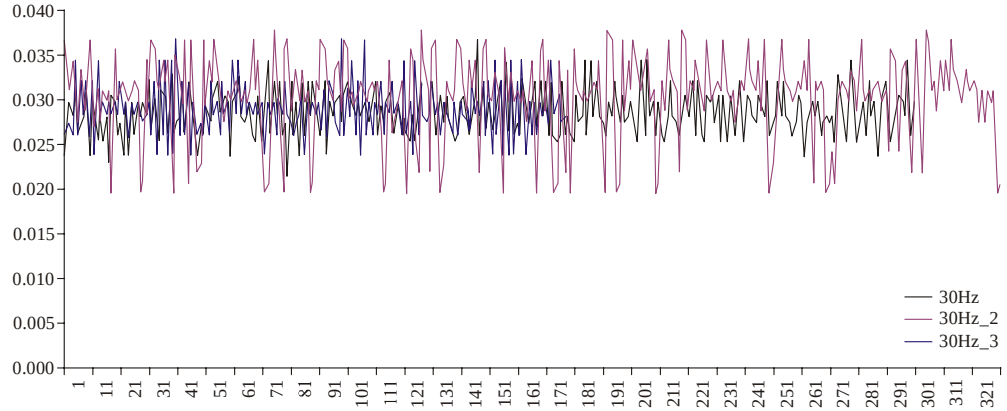

Fig. 20: Lag at 30Hz frequency of oscillation

experiments were conducted for each frequency at the temperatures shown in Fig. 22. For example for the 0.5 Hz, 0.5 Hz legend refers to temperature a, 0.5 Hz_2 is for temperature b and 0,5 Hz_3 is for c respectively. The x-axis indicates the number of data used for the plots. Some outlier data were discarded. From Fig. 21 it is observed that there is progressive drop in the response time as frequency increases. The meaning is that the material becomes softer as the frequency increases. At above 25 Hz, softening becomes more glaring and therefore this particular rubber should not be used above that value for oscillatory motions.

The machine and procedure highlighted in this work show the gradual drop in lag time as the frequency increases. A biomimetic robot joint using rubber as its interconnecting igament will surely fail if the oscillation goes beyond certain value - in this experiment and with this particular rubber sample it is 25 Hz. When the

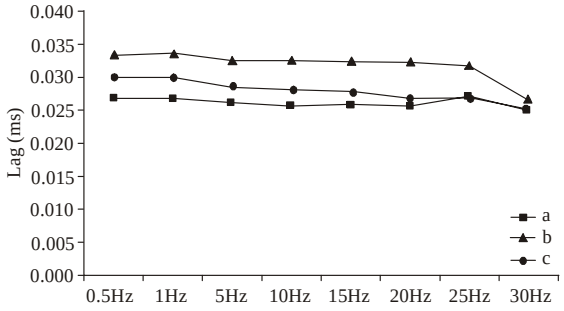

Fig. 21: Progressive drops in response time with increasing frequency. The legend (a,b,c) refers to the environmental temperature

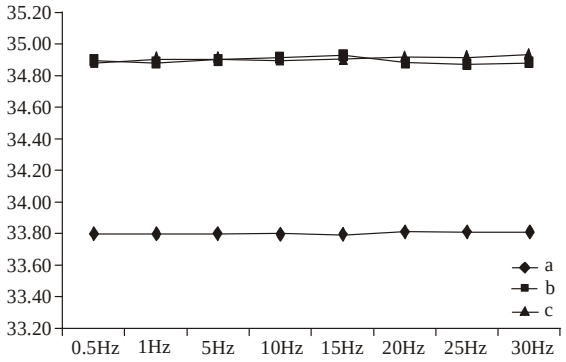

Fig. 22: Different room temperature at which test was carried out. Maximum variation is 1.1°C

Fig. 23: Test on a practical implementation shows a perfect biomimicry of the bending with just two servomotor control cable active. This is a still picture of the video when testing the robotic tail fin

practical model (robotic fish tail/peduncle - Fig. 2) was tested at frequencies of about 2 Hz, the performance in terms of the curvature conform to that of a life fish - it was serpentine in nature also as shown in Fig. 23. This curvature requires very minimal control scheme, only two servomotors were engaged compared to MIT robotuna that uses about six servomotors (Anonymous, 2010d).

CONCLUSION AND RECOMMENDATION

The simplicity so desired in Hyper-redundant robot control system as exemplified by nature is easier to achieve if we look into material used for the robot (especially the joints) itself. The use of rubber here has been shown to be capable of working properly as long as certain frequency value is not exceeded, and a test on a practical model confirms the result.

ACKNOWLEDGMENT

The authors gratefully acknowledge Ahmadu Bello University board of research grant and Macarthur Foundation for their support of this project.

REFERENCES

Anonymous, 2008a. Retrieved from: http://www-robot.mes.titech.ac.jp, (Accessed on: October 24, 2008).

Anonymous, 2008b. Retrieved from: http://www-robot.mes.titech.ac.jp/robot/snake/oblix/oblix_ e.html, (Accessed on: October 24, 2008).

Anonymous, 2010a. Retrieved from: http://world.honda.com/ASIMO/, (Accessed on: August 10, 2010).

Anonymous, 2010b. Retrieved from: http://www.sony.net/Products/aibo/index.html, (Accessed on: August 10, 2010).

Anonymous, 2010c. Retrieved from: http://www.21stcentury.co.uk/ robotics/nomad.asp, (Accessed on: August 10, 2010).

Anonymous, 2010d. Retrieved from: http://web.mit.edu/towtank/www/Tuna/Tuna1/tuna1.html, (Accessed on: September 15, 2010).

Brett, R.F., H.W. William, T. Selim and P.K. Leslie, 2003. A dynamic model of visually - guided steering, obstacle avoidance, and route selection. Int. J. Comput. Vision, 54(1/2/3): 13-34.

Dorfmann, A., B.A. Trimmer and W.A. Woods, 2007. A constitutive model for muscle properties in soft-bodied arthropod. J. Roy. Soc. Int., 4: 257-269.

Grasso, F.W., 2000. Flow - and Chemo-sense for Robot and Lobster Guidance in Odor Source Tracking. Neurotechnology for Biomimetic Robots Conference May-14-16, 2000 at Northeastern University East Point, Nahant, MA 01908.

Gutfreund, Y., T. Flash, Y. Yarom, G. Fiorito, I. Segev and B. Hochner, 1996. Organization of octopus arm movements: a model system for studying the control of flexible arms. J. Neurosci., 16(22): 7292-7307.

Gutfreund, Y., T. Flash, G. Fiorito and B. Hochner, 1998. Patterns of arm muscle activation involved in octopus reaching movements. J. Neurosci., 18(15): 5976-5987.

Harrison, R.R. and C. Koch, 2000. A Silicon Implementation of the Fly Optomotor Control System in Letter by M.V. Srinivasan and Stephen DeWeerth. Neural Computation 12, 2291-2304 (2000) 2000 Massachusetts institute of Technology.

Katsuihiko, O., 2005. Modern Control Engineering. 4th Edn., Publisher Pearson Education Inc., pp: 69-70.

Kevin, J.D., 1997. Limbless Locomotion: Learning to Crawl with a Snake Robot. Ph.D. Thesis, Robotics Institute Carnegie Mellon University, 5000 Forbes Avenue, Pittsburg, PA 15213.

Matsuura, H., M. Mizutame, Y. Moriyama, H. Shimada, S. Hirose and Y. Umetani, 1985. Measuring/grinding system for water turbine runner. Proceeding 2nd International Conference on Advanced Research, pp: 199-206.

Miller, K. and A. Arbor, 2008. Experimental Loading Conditions used to Implement Hyperelastic and Plastic Material Models. Retrieved from: http:// www.axelproducts.com/downloads/ExpLoadings.pdf, (Accessed on: October 23, 2008).

Nagrath, I.J. and M. Gopal, 2005. Control Systems Engineering. 4th Edn., Publisher New Age International Publishers, pp: 194-197.

Ogden, R.W., 2000. Stress Softening and residual strain in the aximuthal shear of a pseudo-elastic circular cylindrical tube. Int. J. Non-linear Mech., Vol. 36.

Ogden, R.W. and D.G. Roxburgh, 1999. A pseudo-elastic model for the Mullins effect in filled rubber. Proc. R. Soc. A., 455: 2861-2877

Park, S.J., M.B. Goodman and B.L. Pruitt, 2007. Analysis of nematode mechanics by piezoresistive displacement clamp. PNAS, 104(44).

Rodney, A.B., 1989a. A Robot That Walks; Emergent Behaviours from Carefully Evolved Network. MIT AI Lab Memo 1091, February 1989. A Book about Genghis. Retrieved from: http://groups.csail.mit.edu/ people/brooks/papers.

Rodney, B., 1989b. Fast, cheap and out of control: Robot invasion of the solar system. J. Br. Interpla. Soc., 42: 478-485.

Shammas, E., A. Wolf, H.B. Brown and H. Choset, 2003. New Joint Design for Three-dimensional Hyper Redundant Robots. Proceedings of the 2005 IEEE International Conference on Robotics and Automation, Las Vegas, Nevada, October.

Srinivasan, M.V., S.W. Zhang, J.S. Chahl, G. Stange and M. Garratt, 2004. An overview of insect-inspired guidance for application in ground and airborne platforms. Proc. Instn. Mech. Engrs., Part G: J. Aerospace Eng., 218: 375-388

Srinivasan, M.V., 1992. Distance Perception in Insects. Centre for Visual Sciences, Research School of Biological Sciences, Australian National University, P.O. Box 475, Canberra, ACT 2601, Australia. Published by Cambridge University Press

Wikipedia Contributors, 2008. Introduction to Biomechanics, Wikipedia, The free Encyclopedia. Retrieved from: http://en.wikipedia.org/w/index. php?title= Introduction_to_ Biomechanics, (Accessed on: October 23, 2008).

Yekutieli, Y., R. Sagiv-Zohar, B. Hahner and T. Flash, 2005. Dynamic model of the octopus Arm II. Control of reaching movements. J. Neurophysiol., 94: 1459-1468.

Yekutieli, Y., R. Sagiv-Zohar, B. Hahner and T. Flash, 2007. Analyzing octopus movements using three-dimensional reconstruction. J. Neurophysiol., 98: 1775-1790.

Zufferey, J.C. and D. Floreano, 2005. Toward 30-gram Autonomous Indoor Aircraft: Vision-based Obstacle Avoidance and Altitude Control. Proceedings of the 2005 IEEE International Conference on Robotics and Automation Barcelona, Spain April 18-22.